



# IGF-axis confers transformation and regeneration of fallopian tube fimbria epithelium upon ovulation

Che-Fang Hsu<sup>a,d,1</sup>, Hsuan-Shun Huang<sup>a,1</sup>, Pao-Chu Chen<sup>b</sup>, Dah-Ching Ding<sup>a,b</sup>, Tang-Yuan Chu<sup>a,b,c,\*</sup>

<sup>a</sup> Center for Prevention and Therapy of Gynecological Cancers, Department of Research, Buddhist Tzu Chi General Hospital, Hualien, Taiwan, ROC

<sup>b</sup> Department of Obstetrics & Gynecology, Buddhist Tzu Chi General Hospital, Hualien, Taiwan, ROC

<sup>c</sup> Institute of Medical Science, Tzu Chi University, Hualien, Taiwan, ROC

<sup>d</sup> Department of Life Science, Institute of Biotechnology National Dong Hwa University, Hualien, Taiwan

## ARTICLE INFO

### Article history:

Received 11 December 2018

Received in revised form 26 January 2019

Accepted 31 January 2019

Available online 7 March 2019

### Keywords:

Ovarian high-grade serous carcinoma

Follicular fluid

Fallopian tube fimbriae

IGF axis

Stemness

## ABSTRACT

**Background:** The fallopian tube fimbria is regarded as the main tissue of origin and incessant ovulation as the main risk factor of ovarian high-grade serous carcinoma. Previously, we discovered the tumorigenesis activity of human ovulatory follicular fluid (FF) upon injection to the mammary fat pad of Trp53-null mice. We also found a mutagenesis activity of FF-ROS and a apoptosis-rescuing activity of Hb from retrograde menstruation. However, neither of them can explain the tumorigenesis activities of FF.

**Methods:** From two cohorts of ovulatory FF retrieved from IVF patients, the main growth factor responsible for the transformation of human fimbrial epithelial cells was identified. Mechanism of activation, ways of signal transduction of the growth factor, as well as the cellular and genetic phenotypes of the malignant transformation was characterized.

**Findings:** In this study, we showed that insulin-like growth factor (IGF)-axis proteins, including IGFBP-bound IGF2 as well as the IGFBP-lytic enzyme PAPP-A, are abundantly present in FF. Upon engaging with glycosaminoglycans on the membrane of fimbrial epithelial cells, PAPP-A cleaves IGF2 and releases IGF2 to bind with IGF-1R. Through the IGF-1R/AKT/mTOR and IGF-1R/AKT/NANOG pathways, FF-IGF leads to stemness and survival, and in the case of TP53/Rb or TP53/CCNE1 loss, to clonal expansion and malignant transformation of fimbrial epithelial cells. By depleting each IGF axis component from FF, we proved that IGF2, IGF2/6, and PAPP-A are all essential and confer the majority of the transformation and regeneration activities.

**Interpretation:** This study revealed that the FF-IGF axis functions to regenerate tissue damage after ovulation and promote the transformation of fimbrial epithelial cells that have been initiated by p53- and Rb-pathway disruptions.

**Fund:** The study was supported by grants of the Ministry of Science and Technology, Taiwan (MOST 106-2314-B-303-001-MY2; MOST 105-2314-B-303-017-MY2; MOST 107-2314-B-303-013-MY3), and Buddhist Tzu Chi General Hospital, Taiwan (TCMMP104-04-01).

© 2019 The Author(s). Published by Elsevier B.V. This is an open access article under the CC BY-NC-ND license (<http://creativecommons.org/licenses/by-nc-nd/4.0/>).

## 1. Introduction

Epithelial ovarian cancer is the fifth leading cause of death among all female cancers and the most fatal among gynecological cancers. Among the various histological types, high-grade serous carcinoma (HGSC) is the most prevalent and devastating one [1], and its etiology is largely unknown.

Contrary to traditional thought on orthotopic origin, increasing evidence has indicated the fallopian tube as the origin of HGSC. Examinations of tubo-ovarian tissues prophylactically removed from high-risk women have revealed precancerous and early cancerous lesions, namely p53 signature, serous tubal intraepithelial lesion (STIL), and serous tubal intraepithelial carcinoma (STIC), exclusively in the fallopian tube, particularly at the fimbrium, which is responsible for oocyte pick-up [2–4]. These lesions universally carry the TP53 mutation with nuclear accumulation of the mutant protein [5]. In addition, many cellular and transgenic mice studies have revealed the main origin of ovarian HGSC to be the secretory cells of the fimbrial epithelium [2,6,7].

Numerous epidemiological studies have suggested that incessant ovulation is a major risk factor for ovarian cancer. Inhibition of ovulation

\* Corresponding author at: Department of Obstetrics and Gynecology, Buddhist Tzu Chi General Hospital, 707, Section 3, Chung-Yang Road, Hualien 970, Taiwan.

E-mail address: [hidrchu@gmail.com](mailto:hidrchu@gmail.com) (T.-Y. Chu).

<sup>1</sup> Equal contribution.

## Research in context

### Evidence before this study

First raised in 1971, the hypothesis for a relationship between incessant ovulation and development of epithelial ovarian cancer has gained increasing support from researchers across various disciplines, even after the paradigm of the tissue-of-origin of ovarian high-grade serous carcinoma had shifted to the fallopian tube. However, direct proof of the carcinogenic activity of ovulation and mechanism of transformation is lacking.

### Added value of this study

This study provides evidence that human ovulatory follicular fluid (FF) is carcinogenic to p53/Rb-deficient fimbrial epithelial cells in vitro and in vivo. FF contains high levels of insulin-like growth factor (IGF)-axis proteins, including IGFBP-bound IGF2 and IGFBP-lytic enzyme PAPP-A. Upon engaging with glycosaminoglycans on the membrane of fimbrial epithelial cells, PAPP-A cleaves IGFs and releases IGF to bind with IGF-1R. Through the IGF-1R/AKT/mTOR and IGF-1R/AKT/NANOG pathways, FF-IGF leads to stemness and survival, and in the case of TP53/Rb or TP53/CCNE1 loss, to clonal expansion and malignant transformation of fimbrial epithelial cells.

### Implications of all the available evidence

This study revealed IGF axis proteins in follicular fluid functions to regenerate tissue damage after ovulation. It also promotes stemness and clonal expansion of fimbrial epithelial cells that have been initiated by p53/Rb disruptions.

by pregnancy and lactation [8,9] and by use of oral contraceptives (OCs) [10] confers a reduced risk of ovarian cancer in a dose- and time-dependent manner. The protection effect is potent enough to be observed even in women with short term (<1 year) anovulation [9–11]. Also, the risk-reducing effect of OCs is long-lasting and does not attenuate until 3 decades after discontinuation of use. This suggests a long-lasting protection effect starting at the cancer initiation stage [11]. A well-designed population-based study further revealed the risk reduction by OCs started as early as 5 years after initiation of use of OCs [11]. Given with a typical developmental course of three decades for cancers, the above epidemiological results suggest a potent carcinogenic effect of ovulation acting in the full course of ovarian carcinogenesis.

We and other scholars [12–15] have proposed that ovulatory follicular fluid (FF), which bathes fallopian tube fimbria after ovulation, may contain transforming carcinogens. A subset of FF retrieved from women receiving in vitro fertilization (IVF) was found to contain high levels of ROS [12]. Exposure of the human fimbrial epithelium to FF induced ROS stress, DNA double-strand breaks (DSB) [12], and upregulation of inflammatory and DNA repair genes [12,14]. Upon repeated, direct injections to the mammary fat pad of Trp53<sup>-/-</sup> mice, the ROS-high FF could induce local tumorigenesis [12]. We also discovered that hemoglobin (Hb) in peritoneal fluids or FF, which most likely was derived from previous retrograde menstruation, could prevent the ROS-stressed fimbrial epithelial cells from apoptotic death [16]. With repeated exposure to ROS-high and Hb-high FF, the fimbrial epithelium showed an expansion of cells with accumulation of DSB [16]. However, neither the mutagenesis effect of ROS nor the apoptosis-rescuing effect of Hb can explain the cell expansion and in vivo tumorigenesis activities of FF. In this study, we discovered that insulin-like growth factor (IGF)-axis in FF is largely responsible for the fat pad tumorigenesis activity as

well as for the clonal expansion and malignant transformation of the human fimbrial epithelium. Two signaling pathways downstream to IGF-1R are responsible for these activities.

## 2. Materials & methods

### 2.1. FF and fallopian tube tissue specimens

FF aspirates were collected from women undergoing an oocyte retrieval and IVF program as described before [12]. Briefly, after HCG injection, ovarian follicles were aspirated vaginally under the guidance of sonography. To minimize flush medium and blood contamination, aspirates of the first trans-vaginal needle introduction, which is typically followed by aspiration of another 2–3 follicles, were harvested. Aspirates with obvious blood contamination were excluded, as revealed through spectrophotometry by absorption of Hb at OD 418 nm. Thirty-one qualified FF aspirates were serially collected and aliquotes were equally pooled for experiments. Fallopian tube tissues were collected from women receiving opportunistic salpingectomy during hysterectomy because of benign causes. Two research programs (TCRD-I102-01-01 and MOST 106-2314-B-303-001-MY2) were involved with approval from the Institutional Review Board of Tzu Chi Medical Center, Taiwan (Approval No. IRB -101-09, IRB -106-07-A).

### 2.2. Human fallopian tube fimbrial epithelial cell lines and treatment with inhibitors

We modified the method reported by Paik et al. for primary culture of human fallopian tube epithelial cells [17]. First, a piece of fimbria tissue was soaked in 1% trypsin and 5 mM EDTA at 37 °C for 30 min; the epithelium of the fimbriae was peeled off, digested with 1.5 mg/ml of collagenase (c2674, Sigma) for 1 h, and cultured in DMEM and 10% fetal bovine serum (FBS) with 5 µg/ml of insulin, 100 IU/ml of penicillin, and 100 µg/ml of streptomycin on a 0.1% gelatin-coated plate. Four immortalized human fimbrial epithelial cell lines were used, namely HPV E6/E7 plus hTERT-transduced FE25 cells [12], p53 R175H, hTERT plus empty vector-transduced FT282-V cells, p53 R175H, hTERT plus CCNE1-transduced FT282-CCNE1 cells [18], and SV40 TAg plus hTERT-transduced FT194 cells [18] (the latter 3 lines were kindly provided by Dr. Ronny Drapkin from the University of Pennsylvania, USA). All cells were maintained in MCDB105 and M199 medium (Sigma) supplemented with 10% FBS and P/S. To test the role of signal transduction pathways in FF-induced cell transformation, the inhibitors of IGF-1R (picropodophyllin, PPP), Ras (farnesylthiosalicylic acid, FTS), AKT (MK2206), and mTOR (rapamycin) were added before the FF.

### 2.3. Fractionization of FF and growth factor array

Pooled FF in 5% was fractionated using Molecular Weight Cut-off (MWCO, Synder Filtration) at 50 kD. The low- and high-molecular weight fractions and the original FF were each subjected to growth factor antibody array using a RayBio® C-Series Human Growth Factor Kit (AAH-GF-1-2, RayBiotech). Two sets of arrays were performed for each sample with consistent results.

### 2.4. RNAi knockdown system

IGF-1R and NANOG in FE25 cells were each knocked down using lentivirus-mediated gene silencing. Target specific sh-IGF-1R (Sequence: GCCTTTCACATTGTACCGCAT), sh-NANOG (Sequence GAGTATGGTTGGAGCCTAATC), and the control sh-Luc (sequence CAAATCACA GAATCGTCGTAT) were obtained from the National RNAi Core Facility (Academia Sinica, Taiwan). Transduced cells were selected with 10 µg/ml of puromycin and subsequently maintained at a reduced dose of 5 µg/ml.

### 2.5. Anchorage-independent cell growth assay

For AIG assay, 4000 cells were suspended in 0.4% agarose and placed on top of 0.8% basal agarose (both prepared in 1 ml culture medium). To test the AIG activity of FF, 100  $\mu$ l of pure FF or control medium was added to the surface of the top gel every 24 h for 2 days with a final concentration of 10% on the top gel; fresh medium was added every 3 days. After 2 weeks, colony formation was imaged using a Nikon Eclipse TS100 microscope and counted using Image J.

### 2.6. Xenograft analysis in NSG mice

To analyze cell transformation, NOD/Shi-scid/IL-2R $\gamma^{\text{null}}$  (NSG) mice (Jackson Laboratory) were used. First, the mice were subcutaneously injected with  $2 \times 10^6$  FE25 cells in a 200  $\mu$ l solution containing 10% Matrigel plus 10% FF or control PBS. In the intraperitoneal injection model, after initial injection of the same FE25 cell +/- FF preparation, 10% matrigel plus 10% FF or PBS was injected every week for a total of 5 weeks. The mice were sacrificed and dissected in the sixth month. All experimental procedures involving mice were conducted under the approved guidelines of the Animal Care and Use Committee of Tzu-Chi University (Approval ID: 105–39).

### 2.7. Tumorigenesis in Trp53 $^{-/-}$ mice by mammary fat pad injection

The method for FF-induced tumorigenesis using mammary fat pad injection was described in a previous report [12]. Briefly, 8-week-old female Trp53 $^{-/-}$  mice (Jackson Laboratory Stock No. 012620) were injected with 5% FF (with or without IGF2 depletion), PBS, or IGF2 (100 ng/ml) at a volume of 200  $\mu$ l into the mammary fat pads every week for a total of 7 weeks before sacrifice.

### 2.8. Immunohistochemistry, immunoprecipitation, and Western blot analysis

For immunohistochemistry (IHC), 4- $\mu$ m-thick paraffin sections were stained with the following primary antibodies: anti-pan CK (sc-15367, Santa Cruz), anti-PAX8 (ab53490, Abcam), anti-WT1 (2797–1, Epitomics), anti-NANOG (GTX100863, Genetex), anti-OCT4 (MAB4305, Millipore), anti-IGF-1R (sc-462, Santa Cruz), and anti-CD3 (sc-20047, Santa Cruz). Next, the sections were incubated with the appropriate secondary antibodies and stained with IHC or immunofluorescence reagents. For the Western blot analysis, a protein extract was resolved in SDS-PAGE, transferred to a nitrocellulose membrane, and detected with anti-AKT (sc-8312, Santa Cruz), anti-pAKT (sc-101629, Santa Cruz), anti-mTOR (sc-517464, Santa Cruz), anti-pmTOR (sc-293133, Santa Cruz) and anti-NANOG (GTX100863, Genetex) antibodies, followed by staining with the appropriate HRP-conjugated secondary antibodies and ECL Western Blot Detection Reagent (GE Healthcare, RPN2209). For IP-Western analysis, anti-IGFBP2 (Santa Cruz, sc-6001) and anti-IGFBP6 (Santa Cruz, sc-6007) (0.2  $\mu$ g/ml) were each mixed with 20  $\mu$ l protein G beads (Santa Cruz, sc-2002) for 1 h before being added to FF and immunoprecipitated overnight at 4 °C. After being centrifuged at 4 °C and washed in PBS 5 times, the pull-down proteins were resolved using 12% SDS-PAGE and subjected to Western blot analysis with anti-IGF1 (Santa Cruz sc-9013) or anti-IGF2 (Genetex GTX60630).

### 2.9. PAPP-A ELISA

The method used for PAPP-A analysis followed the manufacturer's instructions of the Human PAPP-A ELISA Kit (Thermo Fisher Scientific, EHPAPPA). First, the FF aspirates (100  $\mu$ l) with 5-fold dilution by PBS were added to the wells of a 96-well strip plate. Subsequently, they were washed in PBS and detected with PAPP-A antibody, HRP-conjugated secondary antibody, and TMB substrate for chromogenic reaction. Sample quantification against the PAPP-A standard was

performed using an ELISA reader for measuring absorbance at 450 and 550 nm.

### 2.10. Depletion of IGF-axis proteins in FF

For specific depletion of IGF-axis proteins from FF, 25  $\mu$ l protein G beads (Santa Cruz, sc-2002) were incubated with 10  $\mu$ l (0.2  $\mu$ g/ml) of anti-IGF1 (Santa Cruz, sc-9013), anti-IGF2 (Genetex, GTX60630), anti-IGFBP2 (Santa Cruz, sc-6001), anti-IGFBP6 (Santa Cruz, sc-6007), or anti-PAPP-A1 (Santa Cruz, sc-365226) antibodies at 4 °C for 3 h. The antibody-conjugated beads (24  $\mu$ l) were each added to 400  $\mu$ l of FF and rotated overnight at 4 °C. After centrifugation to remove the beads, the supernatants were used for experiments.

### 2.11. Flow cytometry of cell membrane bound PAPP-A

FE25 cells were treated with 5% FF for 10 min, detached with trypsin-EDTA, blocked with cold PBS containing 4% bovine serum albumin, and incubated on ice with PAPP-A monoclonal antibody (sc-365226, 1:150 dilution) for 1 h. After washing in PBS-albumin, the cells were incubated with secondary antibody (sc-3818, 1:200) for 30 min. The cells were then resuspended in ice-cold PBS and analyzed on a flow cytometer (FACSCalibur, BD Biosciences); at least 5000 cells were analyzed. To allow comparison, mean fluorescence intensity values were calculated using CELLQuist and compared with those for a vehicle medium-treated control. For DNA content analysis cellular DNA was stained with propidium iodide before subjected to analysis.

## 3. Karyotyping

Karyotyping of FE25 cell and its derivative cell lines was carried out at the Cytogenetics Laboratory of the Genetics Consultation Center of Tzu Chi Medical Center. Briefly, cells were cultured to reach an exponential growth, arrested at metaphase by adding colchicine, burst by hypotonic solution, fixed on a glass slide, stained with Giemsa dye. Chromosomes were organized in karyograms and reviewed by cytogeneticist. Ten to 15 metaphase spreads were examined in each cell.

### 3.1. 3D spheroid colony forming assay

For the 3-D colony forming assay, a 256-hole mold (3D Petri Dish, Sigma-Aldrich) was used to hold 2% low-melting temperature agarose (Invitrogen). During the preparation, the agarose was maintained at 38 °C. After the agarose had solidified, minimally diluted FE25 cells and primary fibroblast epithelial cells in its regular medium with 10% FBS or serum replacement [containing 25 ng/ml bFGF, 20 ng/ml EGF, 1% ITS Liquid Media Supplement (Sigma-Aldrich, 13146 Sigma) and 1% Antibiotic-Antimycotic (Thermo Fisher Scientific, #15240062)] were seeded on top of the agarose. This preparation provided a non-adhesive and scaffold-free surface to develop and observe spheroid colony. To get a minimal cell number in the holes, 200 cells were loaded to the 256-hole mold. Typically, about 1/4 of the holes contained exactly one cell. Wells containing less or more cells or containing cell cluster were excluded. After cell seeding, the original medium with or without 5% FF was added to the culture daily for two (in experiments with regular serum medium) and three (in experiments with serum replacement medium) days. In the following days, the vaporization volume loss (20  $\mu$ l) was replaced with the original medium every two days. Colonies were observed by taking 40 $\times$  images. Colony forming rate was defined as the proportion of single-cell holes that had developed to the colony of two or more viable cells. The area of the colony was measured and quantitated using Image J.

## 4. Statistics

Statistical analyses were performed with GraphPad Prism software (ver. 5.0c) (GraphPad Software, San Diego, CA, USA). Comparisons of the groups were made by paired Student's *t*-test or unpaired Student's *t*-test. Linear correlations between AIG colony number and PAPP-A level was measured by Pearson correlation coefficient.

## 5. Results

### 5.1. Ovulatory FF-induced malignant transformation in vitro and in vivo

To investigate the transformation activity of FF, four immortalized human fimbrial epithelial cells (FE25, FT282-V, FT282-CCNE1, and FT194) were treated with a pool of 31 ovarian follicle aspirates (FF) from women receiving IVF. These immortalized cells were not fully transformed as indicated by the absence of anchorage-independent growth (AIG) in soft agar and absence of tumorigenesis in xenograft (Fig. 1a, b). By contrast, AIG was induced in all cells after treatment with 5% FF (Fig. 1a). The size of the grown colony was compatible with the severity of oncogenic disruption in cells. Colonies of cells expressing a less severe oncogene (SV40 Tag in FT194) or carrying only one disrupted tumor suppressor gene (TP53-R175H in FT282V) were smaller, whereas those of cells transduced with HPV E6/E7 (FE25) or disrupted with both TP53 and CCNE1 (FT282-CCNE1) were larger. When the FF was heat-inactivated, colony number was largely decreased (Fig. 1a). Xenograft tumorigenesis was also induced by FF. Upon injection with FE25 cells together with 10% FF, 7 of 11 (64%) and 4 of 9 (44%) NSG mice grew tumors at subcutaneous and intraperitoneal sites, respectively. Subcutaneous tumor became palpable at 4 months. The intraperitoneal growths were evident at 6 months, locating at the peritoneum/omentum, the intestinal mesenter/serosa, the ovary and the uterus in 3/4, 4/4, 3/4 and 1/4 mice, respectively. The same co-injection of FT282-CCNE1 cells also led to the growth of subcutaneous tumors in 6 of 8 (75%) mice (Fig. 1b). These tumors showed histology of poorly differentiated carcinomas positive for pan-CK and Pax8 and focally expressed WT1 (Fig. 1c). IGF-1R was also highly expressed in these tumors (this is described in detail later). By contrast, no tumor growth was noted at subcutaneous and intraperitoneal sites in 11 and 6 mice injected with FE25 cells alone, respectively. Given that TP53 mutations are the universal early hit of virtually all HGSCs, we tested the transformation activity of FF by direct injection to the mammary fat pad of *Trp53*<sup>-/-</sup> mice, which spontaneously grew lymphomas in old age (median 19.5 ± 4.6 weeks) [19]. When FF (5%) was injected weekly for up to 7 weeks, 3 of 6 (50%) mice developed CD3+ T cell lymphoma by age 14 weeks, whereas none of the 6 mice injected with the vehicle grew tumors (Fig. 1c–d).

### 5.2. IGFBP-bound IGF in FF was responsible for the transformation activity

To identify the molecules responsible for the transformation activity, we conducted protein fractionation, growth factor array, and AIG analysis on FF. Among the 41 molecules in the array, three IGF-binding proteins (IGFBP2, IGFBP6, and IGFBP1), one growth factor (hepatocyte growth factor; HGF) and two secreted receptors (M-CSFR and AR) were abundantly present in FF (Fig. 2a). These proteins were all included in the high (>50 kD) molecular weight fraction, which conferred the majority of the AIG activity (33 colonies vs. 3 colonies in the <50 kD fraction) (Fig. 2a). IGFBPs are known to trap IGF until when they are cleaved by PAPP-A or other proteases and release IGF in the vicinity of the target cell [20]. To examine whether IGFs or HGF in FF is responsible for the transformation, we tested their specific inhibitors on the transformation activity of FF on FE25 cells. Whereas inhibition of IGF-1R with picropodophyllin (PPP) dose-

dependently reduced the >25 μm AIG colony number, inhibition of the HGF receptor had only a modest effect (Supplementary Fig. 1). Thus, we considered the IGF axis as the main carcinogen in FF. Indeed, knockdown of the *IGF-1R* gene in FE25 cells resulted in a complete loss of FF-induced AIG and tumorigenesis (Fig. 2b–c, Supplementary Fig. 2). In addition, AIG could be directly induced by IGF1 or IGF2 but only moderately by insulin, an alternative ligand of IGF-1R with less affinity and lowly expressed in FF (Fig. 2b).

Because free-form IGFs were only scarcely present in our array analysis of FF, we wondered whether they were bound by IGFBPs. Indeed, by immunoprecipitation–Western blot analysis, we found that both IGFBP2 and IGFBP6 carried abundant IGF2 but little IGF1 (Fig. 2d). Using antibody depletion, we further tested the contribution of each member of IGF-axis proteins in FF-induced transformation. As shown in Fig. 2e–g, AIG was largely reduced when IGF2, IGFBP2, IGFBP6, or PAPP-A was depleted from FF, whereas depletion of IGF1 only showed a modest effect (Fig. 2e). In the FE25 + FF xenograft and/or Trp53-null fat pad injection models, depletion of IGF2 or PAPP-A also showed a two-third decrease in tumorigenesis rates (Fig. 2f and g). These results indicate that IGFBP-bound IGF2 in FF is responsible for the transformation activity.

### 5.3. FF-IGF transformed through the IGF-1R/AKT/mTOR pathway

The signaling pathway downstream of IGF-1R in FF-induced transformation was further characterized. After treating with FF, there was a quick autophosphorylation at 3 min (Supplementary Fig. 3), followed by phosphorylation of AKT and mTOR at 30 min in FE25 cells but not in cells with IGF-1R knockdown (Fig. 3a). This rapid phosphorylation was also observed in ex vivo cultured human fimbrial tissue after FF treatment (Fig. 3b). In the cases of FE25 cells treated with FF with individual IGF axis components being depleted, the same extent of decreases in AIG occurred as the decreases in AKT/mTOR phosphorylation (Figs. 3c and 2e), which indicated that the signal transduction correlated with the transformation activity. Furthermore, inhibition of IGF-1R, AKT, and mTOR resulted in 100%, 92%, and 80% losses of AIG activity, respectively (Fig. 3d). Meanwhile, the alternative Ras/MEK/ERK pathway downstream of IGF-1R was not operating because inhibition of RAS with farnesylthiosalicylic acid (FTS) did not alter the AIG of FE25 cells (Fig. 3d).

### 5.4. Upon tethered to glycosaminoglycan on the membrane of fimbrial epithelial cells, FF PAPP-A released IGFBP-bound IGF2 for action

Among the IGF-axis proteins tested in FF, depletion of the IGF cleavage enzyme PAPP-A resulted in the largest reduction of AKT/mTOR phosphorylation (Fig. 3c) and FF-induced transformation (Fig. 2e, f). To activate its protease activity, PAPP-A must bind to heparin sulfate glycosaminoglycan (GAG) on the membrane of the target cell [21,22]. Indeed, we found an increase in membrane-bound PAPP-A on FE25 cells 10 min after treatment with FF, which could be completely abolished when the GAG-docking sites were blocked by pretreatment with heparin (Fig. 3e). Heparin treatment also largely reduced the FF-induced AIG activity (Fig. 3f). Also, we ruled out the fimbrial epithelium as the source of PAPP-A because only IGF-1R but no PAPP-A was detected in the fimbrial tissue (Supplementary Fig. 5). Given this critical role of PAPP-A, we analyzed the relationship between PAPP-A levels and AIG activity in another set of 30 FF aspirates and found a high correlation ( $R^2 = 0.36$ ) between PAPP-A concentration and transformation activity (Fig. 3g). Levels of other IGF axis proteins in FF, including IGF2 ( $R^2 = 0.29$ ), IGFBP2 ( $R^2 = 0.27$ ) and IGF1 ( $R^2 = 0.18$ ), also correlated with the AIG activity to a less extent (Supplementary Fig. 4). Thus, the amount of PAPP-A in FF is critical for IGF signaling in transformation

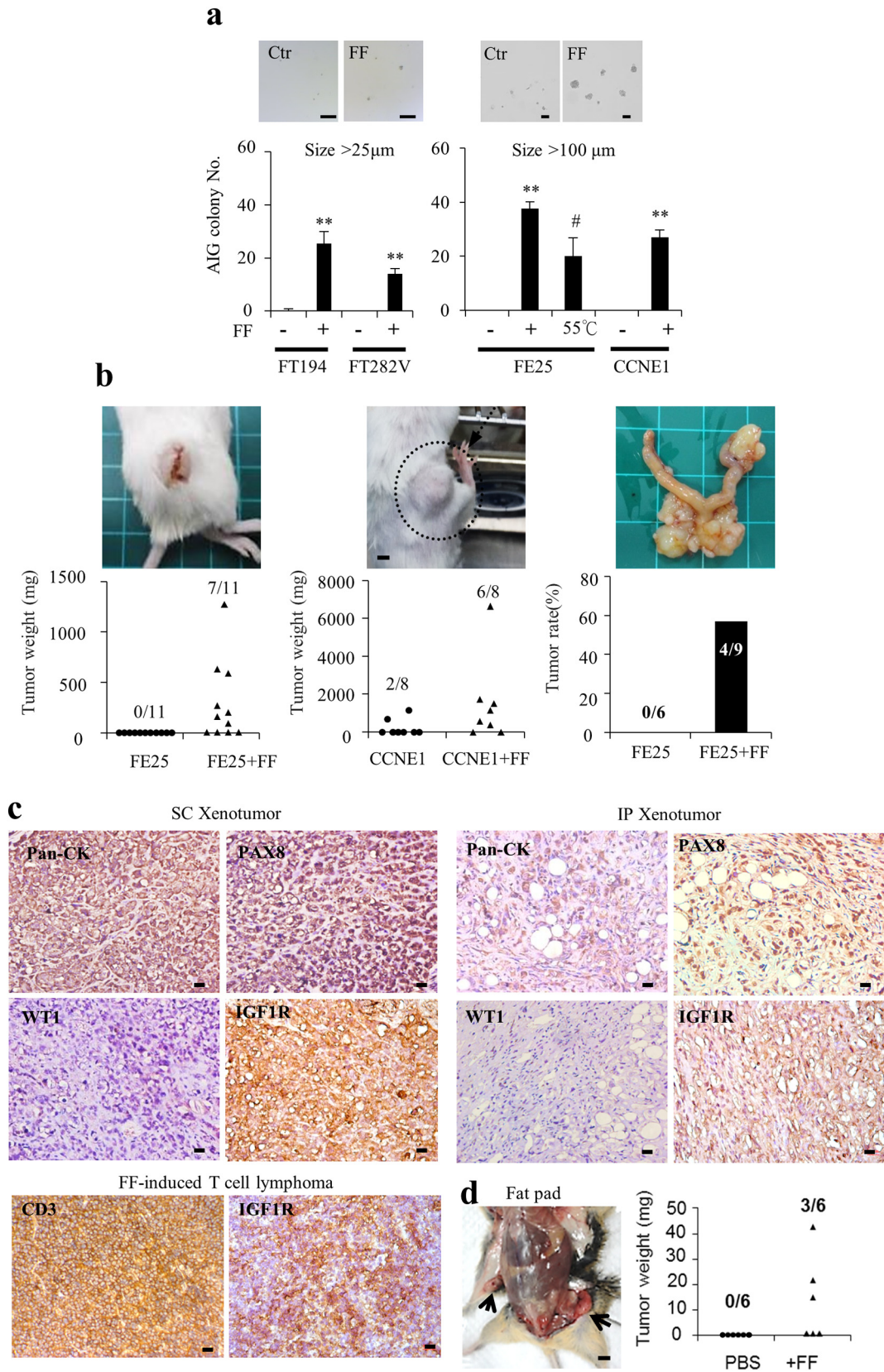


**Fig. 1.** Ovulatory FF could transform immortalized human fimbrial epithelial cells. (a) Four immortalized human fimbrial epithelial cells were treated with 5% FF from a pool of 31 IVF aspirates or vehicle with or without heat inactivation at 55 °C 30 min and subjected to the AIG assay. Representative colonies of >25 µm and >100 µm sizes are shown (scale bar: 100 µm). Results are from three independent experiments. (b) Female NSG mice were injected subcutaneously (SC) or intraperitoneally (IP) with  $1 \times 10^6$  FE25 or FT282-CCNE1 cells in 10% matrigel, with or without a supplement of 10% FF, and sacrificed in the sixth month. Representative gross pictures and tumor incidence/weight are shown. (c) IHC staining of xenograft tumors (scale bar: 20 µm). (d) FF (5% in 200 µl PBS) or PBS alone was injected directly to the mammary fat pad once a week for 7 weeks in Trp53-null mice. Representative pictures of local tumors (arrows) and IHC staining, as well as tumor weights are shown.

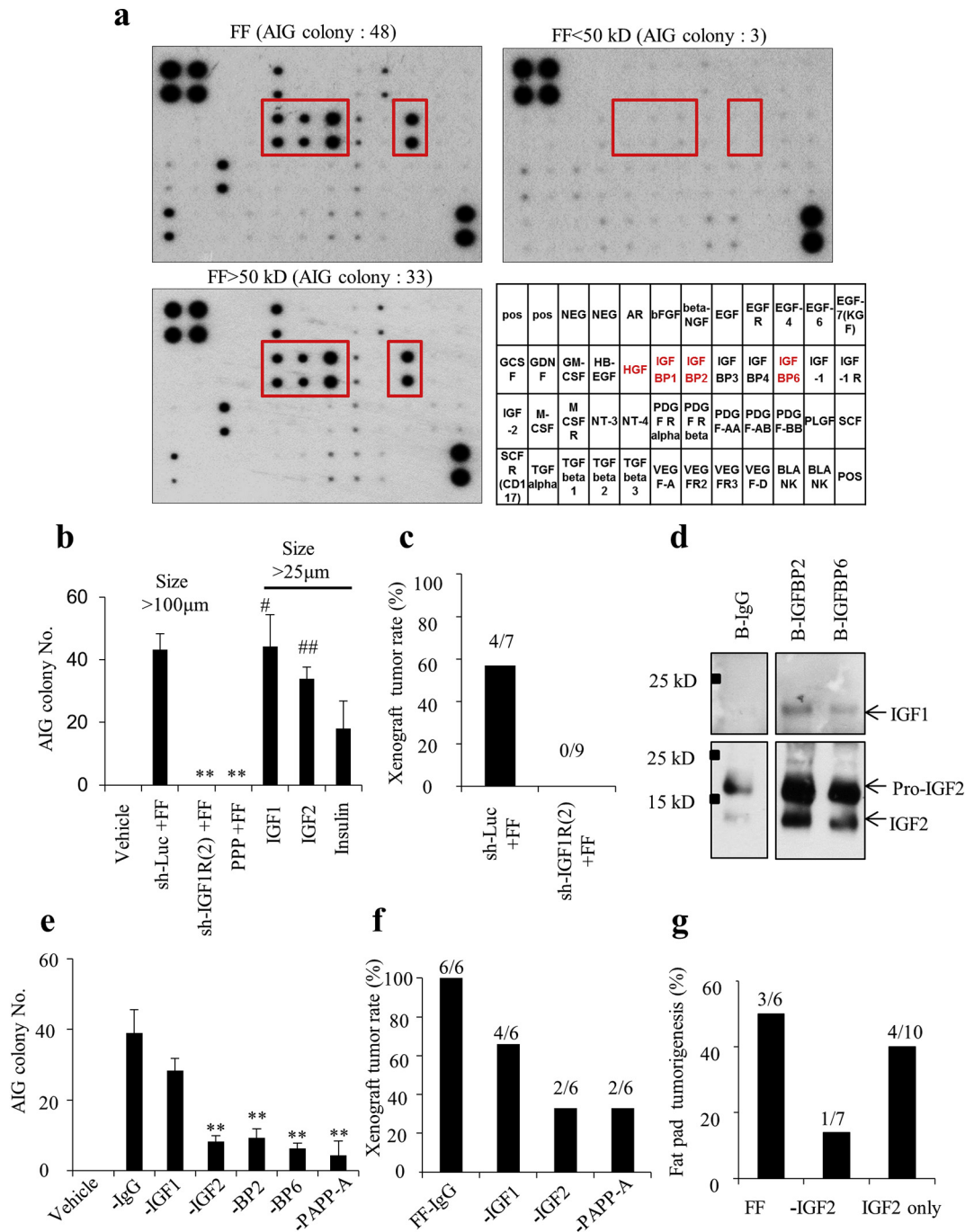


**Fig. 2.** IGFBP-bound IGFs in FF are responsible for FF transformation activity. (a) Growth factor array of FF with or without molecular size fractionation; abundantly expressed growth factors are boxed. AIG colony numbers of FF-treated FE25 cells are given. (b) AIG of FE25 cells with or without IGF-1R knocked down were treated with IGF1, IGF2, Insulin, 5% FF or vehicle. (c) Tumorigenesis in NSG mice after subcutaneous coinjection of 10% FF and FE25 cells with or without IGF-1R knocked down. (d) IP-Western analysis of IGF1 and IGF2 in FF precipitated with bead-conjugated antibodies against IGFBP2, IGFBP6 or IgG control. (e, f) AIG (e) and xenograft tumorigenesis (f) of FE25 cells treated with FF depleted of IGFs (-IGF1, -IGF2), IGFBPs (-BP2, -BP6), the IGFBP cleavage enzyme (-PAPP-A). (g) Tumorigenesis rates of FF, IGF2-depleted FF and IGF2 (100 ng/ml in 200 µl PBS) in the FF-fat pad injection model in Trp53-null mice.

when the enzymatic activity is activated by GAG-tethering on the target cells.

#### 5.5. FF-IGF induced stemness through the IGF-1R/AKT/NANOG pathway

The cellular mechanism of transformation by FF-IGF was further analyzed. We found that although FF moderately increases proliferation of FE25 cells, depletion of IGF axis components from FF did not alter the proliferation (Supplementary Fig. 6a). Treatment with

recombinant IGF2 protein also did not increase the survival of cells stressed with ROS (Supplementary Fig. 6b). However, the stemness of the cells (i.e., nuclear translocation of OCT4 and nuclear expression of NANOG) was readily induced by FF or IGF2 treatment in FE25 cells and could be abolished by cotreatment with the AKT inhibitor MK2206 (Fig. 4a). Among them, AKT phosphorylation and OCT4 translocation were observed as soon as 5 min after FF treatment and were followed by a progressive nuclear expression of NANOG starting from 24 h to 72 h (Fig. 4b, c). By contrast, when IGF-1R was knocked down

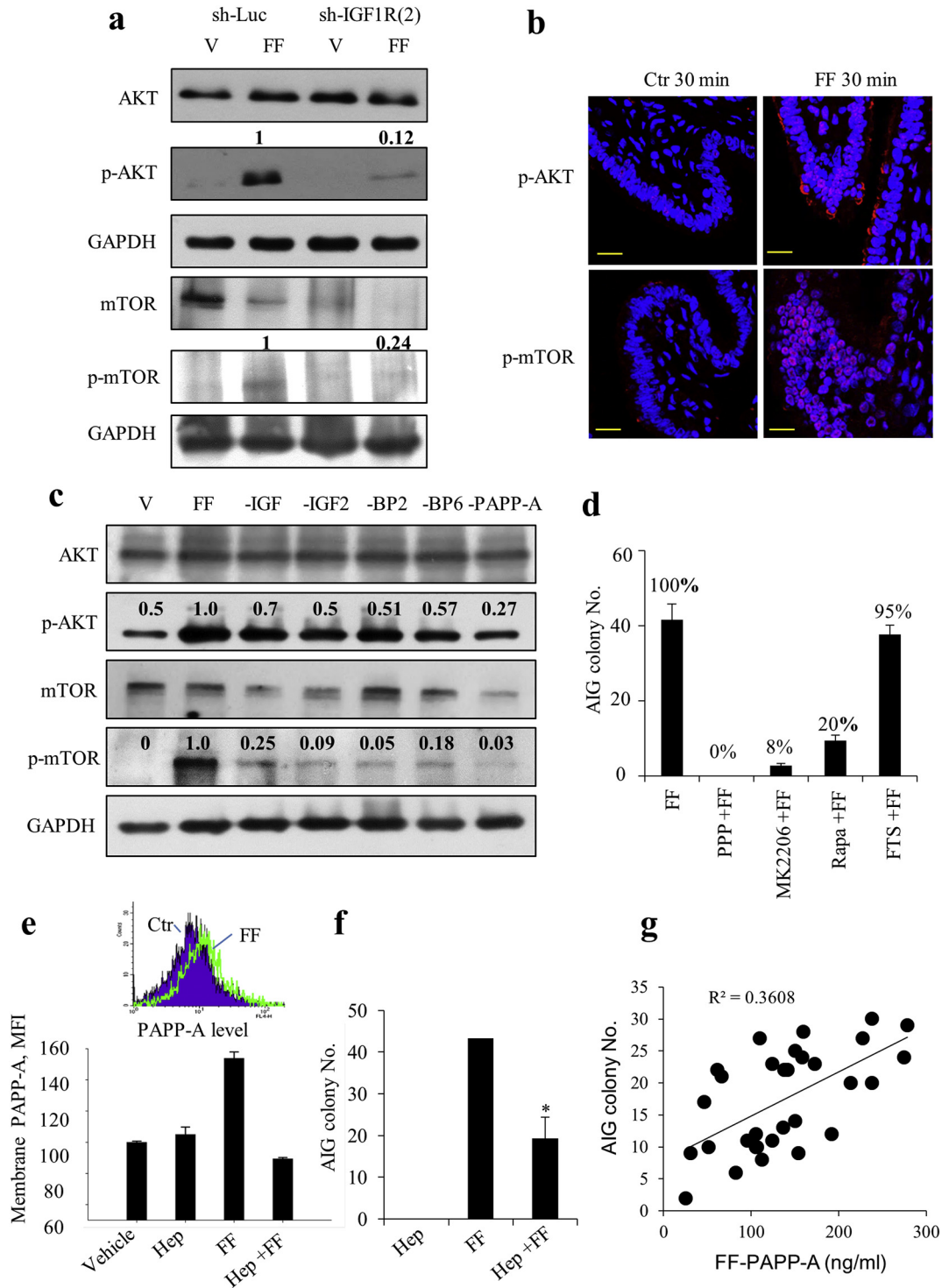


**Fig. 3.** FF-IGF transforms FE25 cells through the IGF-1R/AKT/mTOR pathway. (a) Expression of AKT, mTOR and their phosphorylated (p) proteins in FE25 with (sh-IGF1R(2)) or without (sh-Luc) IGF-1R knocked down were treated with 5% FF for 30 min. The relative densities of bands are given. (b) Ex vivo cultured human fimbrial tissues were treated with 100% FF or control medium for 30 min and subjected to fluorescence immunostaining for p-AKT and p-mTOR. Scale bar: 20  $\mu$ m (c) FE25 cells were treated with FF with or without depletion of IGFs (-IGF1, -IGF2), IGF1R inhibitors (-BP2, -BP6), and PAPP-A for 30 min and subjected to Western blot analysis. (d) AIG of FE25 cells after the same FF treatment following pretreatment (1 h) with inhibitors of IGF-1R (PPP, 5  $\mu$ M), AKT (MK2206, 10  $\mu$ M), mTOR (rapamycin, Rapa, 10  $\mu$ M), or RAS (FTS, 10  $\mu$ M). (e, f) Flow cytometry of cell membrane-bound PAPP-A (e) and AIG assay (f) of FE25 cells after the same FF treatment with or without pretreatment with 100  $\mu$ g/ml of heparin for 10 min. (g) Scatter plot of PAPP-A levels of 30 FFs and AIG colony numbers of FE25 cells induced by each FF with correlation coefficient provided.

in FE25 cells or IGF2 was depleted from FF, a marked decrease in NANOG expression occurred (Fig. 4c), indicating that IGF2 signaling is largely responsible for FF-induced stemness. The importance of this stemness property in the transformation was further characterized. Knockdown of NANOG resulted in decreases in AIG in a dose-

dependent way with a nearly complete loss in the most severe clone (Fig. 4d).

In addition, we wondered whether the stemness induction activity of FF worked in the normal fimbrial epithelium. In ex vivo cultured human fimbrial tissue, the same induction of stemness markers of

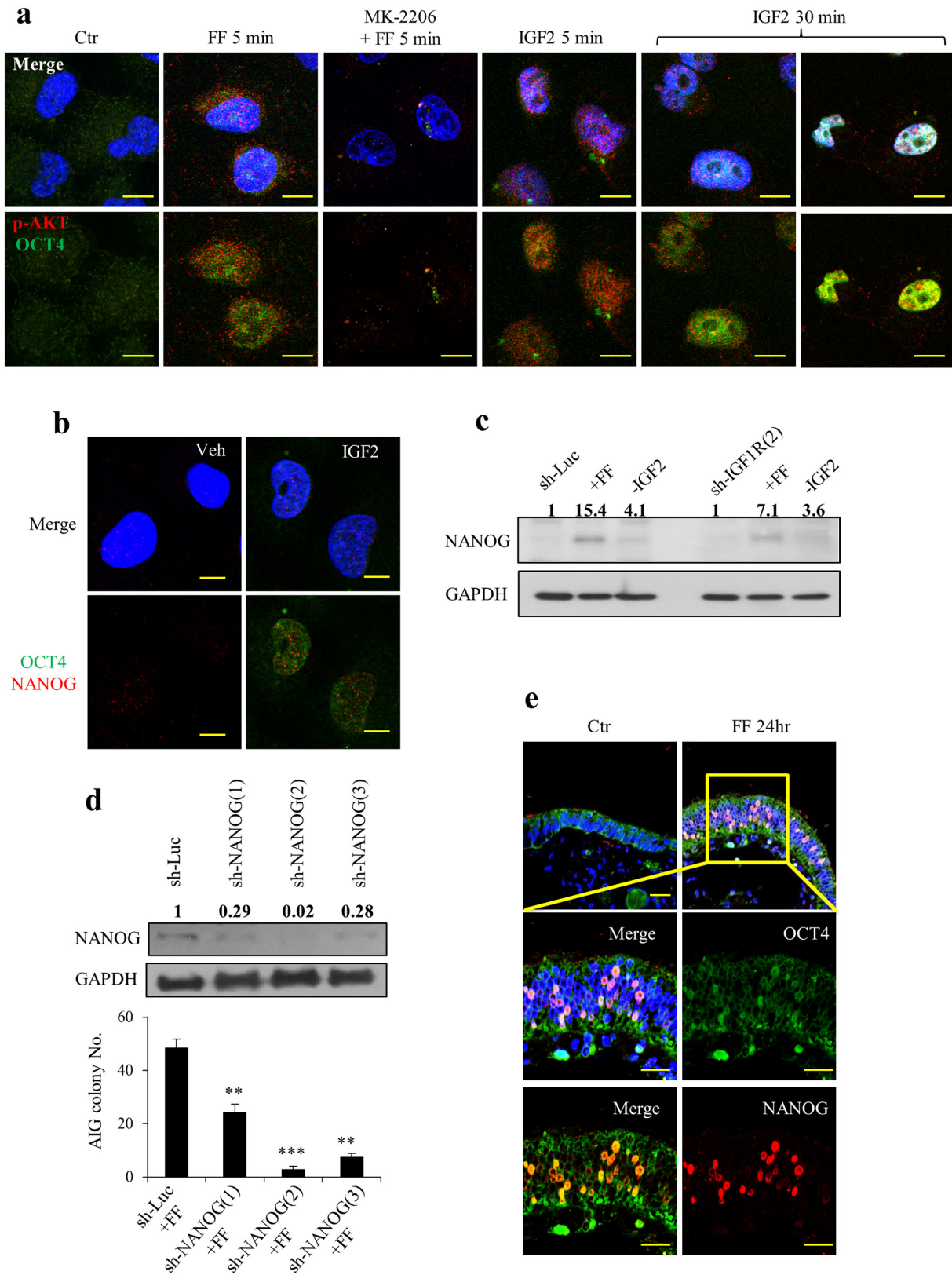


**Fig. 4.** FF-IGF induces stemness of normal and immortalized fimbrial epithelial cells. (a) FF-IGF induces phosphorylation of AKT by 5 min and nuclear translocation of OCT4 by 30 min in FE25 cells. Cells were pretreated or not pretreated for 24 h with 10  $\mu$ M of AKT inhibitor (MK2206), followed by treating with 10% FF or 100 ng/ml IGF2, fixed at 5 min and 30 min, and examined by immunocytochemistry of p-AKT (red) and OCT4 (green). Representative pictures are showed. (b) Nuclear expression of OCT4 and NANOG were observed 24 h after treating FE25 cells with IGF2. (c) Western blot analysis of NANOG expression in FE25 cells with or without IGF-1R knocked down at 24 h after treatment with vehicle or FF with (-IGF2) or without depletion of IGF2. (d) Western blot analysis of 3 clones of FE25 cell with NANOG knocked down (left), and AIG assay after the same treatment with FF (right). (e) The same OCT4 translocation and NANOG nuclear expression were examined in ex vivo cultured fimbrial tissues after the same FF or vehicle treatment for 24 h. Scale bar: 10  $\mu$ m.

OCT4 nuclear transport and NANOG expression was observed after FF treatment (Fig. 4e).

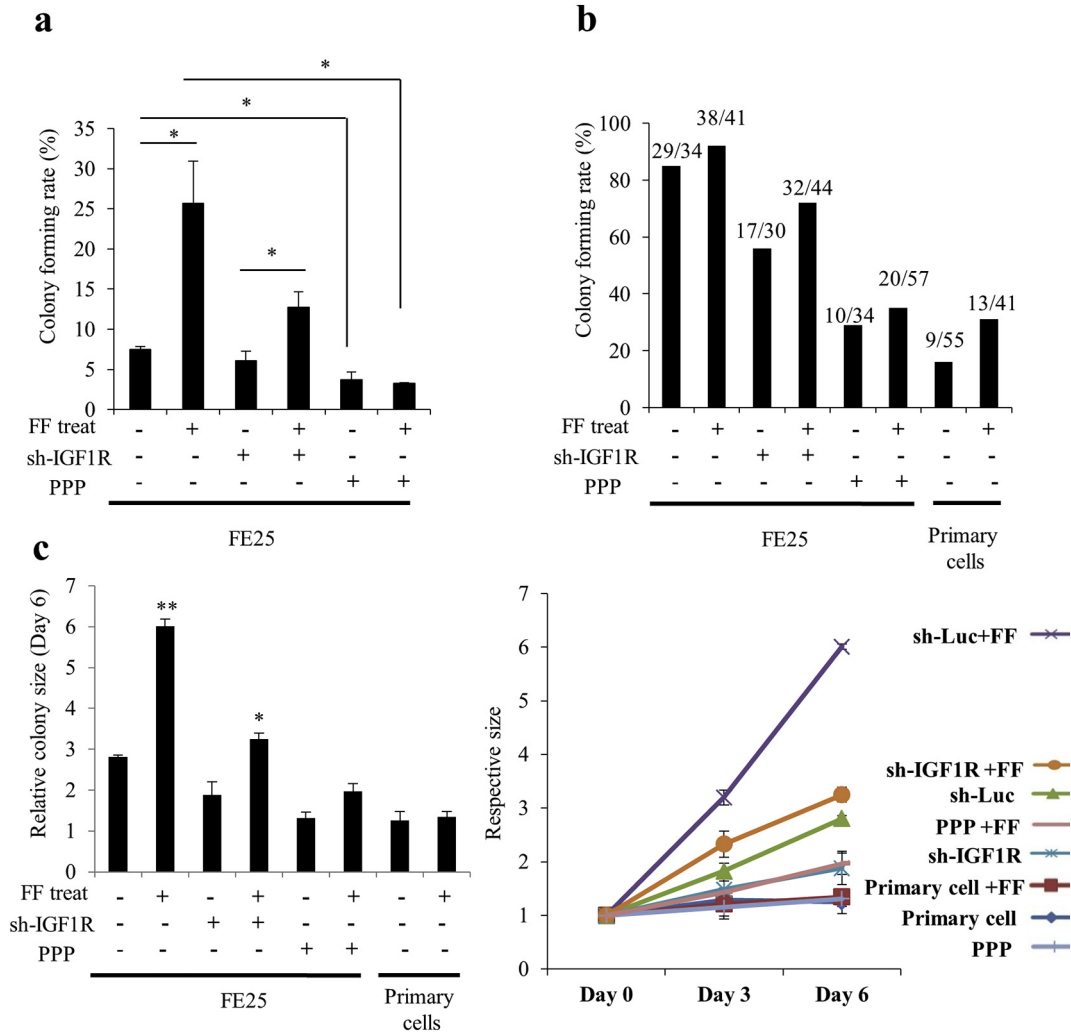
### 5.6. FF-IGF axis signaling induced clonogenicity and clonal expansion of fimbrial epithelial cells

Fig. 5 showed the effect of FF-IGF on clonal development of primary fimbrial epithelial cells grown in 3D spheroid culture. After 10 days culture in serum replacement medium, 7.5  $\pm$  0.4% of single cell clones from FE25 cells developed to a colony. FF treatment markedly increased the rate to 25.7  $\pm$  5.2%. When IGF-1R was impaired by shRNA or PPP, there was a markedly decrease of the colony forming rates in both FF-treated and untreated cells (Fig. 5a). In contrast to a morphology of clear and loose colony with expanded cells, the IGF-1R-impaired colonies were smaller and more condensed with compacted cells. This phenotype was partially reversed after FF treatment (Supplementary Fig. 7a). In order to observe the effect on clonal expansion, the same experiment was done in 10% FBS. A large increase of the basal rate of colony formation (85.3% vs. 7.5%) and colony size (Supplementary Fig. 7b) was noted; FF further increased the colony forming rate to 92.7% and dramatically increased the colony size, which again largely depended on an intact function of IGF-1R (Fig. 5b, c). Importantly, although unable to form a colony on serum replacement medium, 16% (9/55) of the

single cell clones of primary fimbrial epithelial cells grew to colony under regular serum culture. FF treatment doubled the colony forming rate but could not support the growth of a larger colony (Fig. 5c). Since only stem or progenitor cells can form colonies in 3D culture, the results suggest IGF axis in FF confers a stem cell activation activity in fallopian tube fimbrial epithelium. In the p53/Rb-inactivated FE25 cells, FF-IGF further induces expansion of the stem cell clones.

### 5.7. FF-induced transformation of FE25 cells involves the accumulation of chromosomal aberrations and copy number variations (CNVs)

The stemness induction and clonal expansion of FE25 cells showed above do not explain the underlying mechanism of malignant transformation at the genetic level. We conducted DNA content analysis and karyotyping of the transformed xenograft tumor cells as well as the parental lines at different passages. As showed in Fig. 6 and Table 1, the E6/E7/hTERT-immortalized FE25 cells at passage 31 showed a subdiploid DNA content and chromosome count. The composite karyotype from 10 metaphases gave 5 derived chromosomes and 3 marker chromosomes involving chromosomes 8, 9, 11, 15, 16, 17, 21, and 22. The chromosome numbers ranged from 42 to 43. At passage 115, a new polyploid population with 74–77 chromosomes arose in addition to the subdiploid one with 39–40 chromosomes. While both karyotypes



**Fig. 5.** FF-IGF signaling is responsible for the clonal expansion and/or colony formation of fimbrial epithelial cells under 3D spheroid culture. Under the 3D spheroid culture in serum replacement medium (a) or regular serum medium (b, c) with or without FF treatment and IGF-1R impairment, colony formation and expansion from primary and E6/E7-immortalized fimbrial epithelial cells were observed. IGF-1R was knocked down by shRNA (sh-) or inhibited with PPP (1  $\mu$ M). (a) Colony forming rates on day 10 with serum replacement culture. (b) Colony forming rates on day 6 of regular serum culture. (c) Relative size (compared to that of day 0) of colonies on day 6 (left panel) of regular serum culture. The right panel shows the trend of increase on day 0, 3 and 6.

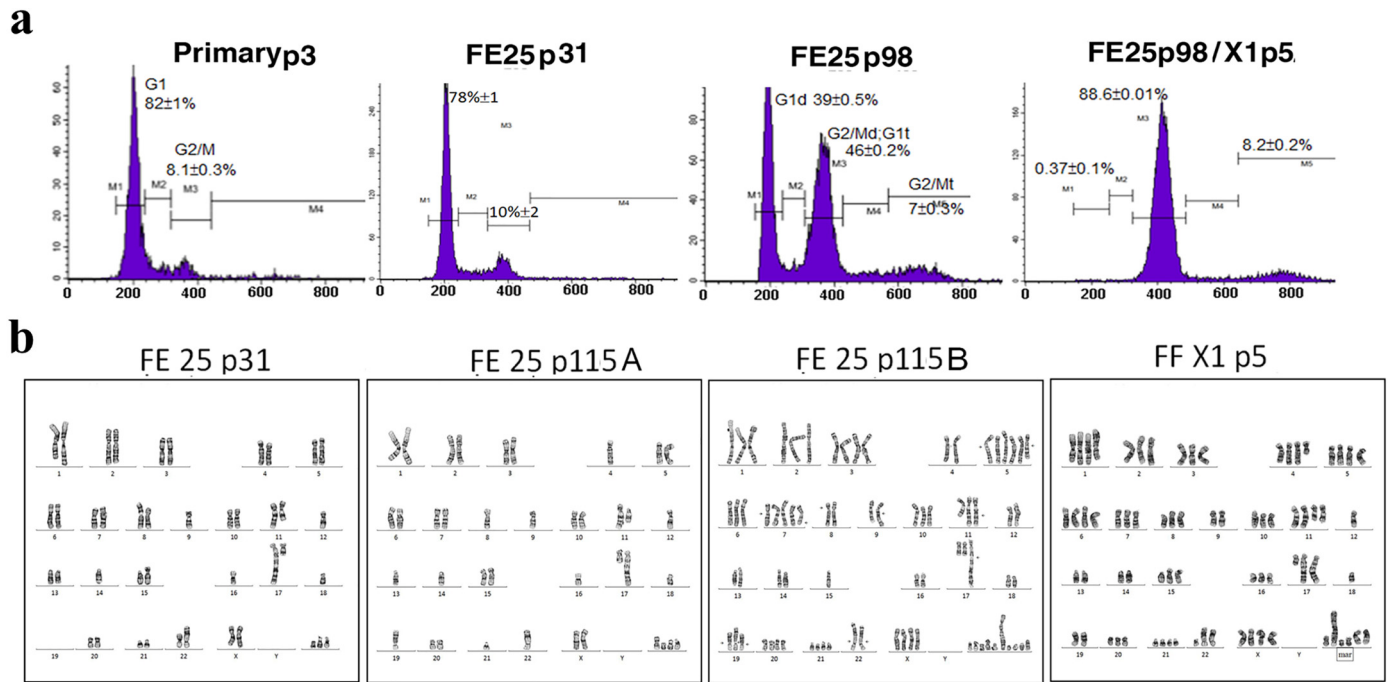


**Fig. 6.** and **Table 1.** Accumulation of chromosomal aberrations and DNA aneuploidy in FE25 cells and exacerbation in FF-induced tumorigenesis. DNA content and karyotypes of FE25 cells of different passage, as well as the derived xenograft tumor cells induced by FF (FE25 p98/X1) were characterized by flow cytometry and G banding. Shown are a representative karyotype from 15 metaphases of FE25 p31, 10 metaphases from FE25 p98/X1 and 5 each from the two distinct subclone (a and b).

differed from that of the earlier passage, more extensive chromosomal changes were noted in the polyploid population. The numbers of derived/marker chromosome increased to 5/4–6 and 8/7–10, respectively. These CNVs and chromosomal aberrations became even more severe in the xenograft tumor cells transformed by FE25 p98 and FF coinjection. In addition to the 5 derived chromosomes inherited from the parental lines, we observed 6 new derived chromosomes and one deletion within the polyploid karyotypes containing 67–76 chromosomes. Also, a relatively monotonous pattern of DNA content was observed in the tumor cells. These results indicate a spontaneous evolution of chromosomal aberrations and CNVs during the passage and FF-induced transformation of the p53/Rb deficient FE25 cells.

## 6. Discussion

First raised in 1971 by Fthalla [23], the hypothesis for a relationship between incessant ovulation and development of epithelial ovarian

cancer has gained increasing support from researchers across various disciplines, even after the paradigm of the tissue-of-origin had shifted to the fallopian tube [24]. However, direct proof of the carcinogenic activity of ovulation and mechanism of transformation is lacking. This study provides evidence that human ovulatory FF is carcinogenic not only to p53/Rb-immortalized fimbrial epithelial cells with the p53 loss but also in fat pad tissue of *Trp53*-null mice. Fig. 6a summarized the mechanism of transformation. After ovulation, the fimbrial epithelium is exposed to IGF-axis proteins in FF. Upon encountering the fimbrial epithelial cells, PAPP-A is activated to cleave IGFBPs and release IGF2. Through IGF-1R and the downstream AKT/mTOR and AKT/NANOG pathways, the IGF signal leads to stemness activation, clonal expansion, and malignant transformation. Specifically, stem cells that have acquired driver mutations may be the target of expansion. Indeed, a spontaneous gain of CNVs and chromosome aberrations underlies the evolution of FE25 cells in culture, and the subline from the FF-induced xenograft tumor showed triploid karyotypes with severe CNVs and

**Table 1**  
Composite karyotypes of FE25-derived cell lines.

Cell type	Chr. No.	Chr. 1	Chr. 3	Chr. 4	Chr. 5	Chr. 8	Chr. 9	Chr. 10	Chr. 11	Chr. 15	Chr. 17	Chr. 19	Chr. 22	Chr. 23	Mar Chr.
FE25 p31	42~43 (n=15)					der(8)t(8;?) (p10;?)			der(11)t(9;11) (q13;q23)	der(15)t(15;21) (p10;q10)	der(17)t(17;?) (q25;?)		der(22)t(16;22) (q11.2;p11.2)		3
FE25 p115 A	39~40 (n=5)								del(11) (p11.2)	der(15)t(15;21) (p13;q11.2)	der(17)t(17;?) (q25;?)	der(19)t(19;?) (p11;?)	der(22)t(22;?) (p11.2;?)		4~6
FE25 p115 B	74~77 (n=5)			der(4)t(4;7) (p10;p10)	+der(5)t(5;7) (q13;q11.2)		der(9)t(9;?) (q21;?)	der(11)t (11;?)q24;?)		der(15)t(15;21) (p13;q11.2)	der(17)t(17;?) (q25;?)	der(19)t(19;?) (p11;?)	der(22)t(22;?) (p11.2;?)		7~10
FE25 p139	59~74 (n=15)					der(8)t(8;C 11)(p10;?)		der(11)t(9;1 1)(q34;q23)		der(15)t(15; ? 5 )q10; ? p10)	der(17)t(17; ? ; 11;9)		der(22)t(22; ? )p10; ? X2,		5~13
FE25 p98/X1	67~76 (n=10)	der(1)t(1;10) (p10;q10)	der(3)t(3;?) (q11.1;?)	del(4)(q25)		der(8)t(8;?) (p11.2;?)	der(9)t(9;12) (p10;q10) der(9)t(9;17) (p10;q10)		der(11)t(11;?) (q24;?)x2	der(15)t(15;21) (p13;q11.2)x2	der(17)t(17;?) (q25;?)x2	der(19)t(19;?) (p11;?)x2	der(22)t(22;?) (p11.2;?)x2	der(X)t(X;?) (q26;?)	6~8

\*Shown are composite karyotypes based on 5, 10 or 15 metaphases (number showed in parentheses) of analyzed cell type

\*\*Derived chromosomes inherited from the parental FE25 p31 cell were marked in green, those developed in p115 were marked in blue, and those from FF-induced xenograft tumor in orange.

DNA aneuploidy. Cell polyploidy reportedly leads to cell cycle arrest at the 4 N G1 checkpoint [25] and the mitotic spindle assembly checkpoint at M phase [26], which requires intact p53 and Rb function, respectively [27]. With the loss of p53 and Rb pathways, FE25 cells as well as early lesions of HGSC [28] skip over these cell cycle checkpoints and lead to severe chromosomal instability and aneuploidy [29].

The importance of the IGF axis in the development of ovarian cancer is highlighted by epidemiological studies. In an analysis from a pool of 12 cohorts, body height was found positively associated with ovarian cancer risk [30]. Large scale GWA studies also found IGF2 related genes including *IGF2BP2*, *IGF2BP3*, *PAPPA*, *PAPPA2*, and *IGF1R* represent important loci associated with adult height [31]. By depletion experiments, we found each of the key components of the IGF axis, including IGF2, IGFBP 2/6, PAPP-A, and IGF-1R, is essential for the transformation. This is due to the most majority of IGFs in FF are bound by IGFbps.

In contrast to IGF1 which is the main growth hormone in all adult tissues, IGF2 is the growth hormone in the fetus and ovarian follicle [32–34]. In agreement with previous studies, we found IGF2 is much more abundant than IGF1 in FF [35,36]. We also found this high IGF2 confers the majority of FF transformation activity. The majority of them were bound to the two IGF2-preferent binding proteins, IGFBP2 and IGFBP6, which counteract its activity by preventing its interaction with the receptor [37,38]. The IGFBP2-cleavage enzyme PAPP-A is also abundantly present in FF. All these IGF axis proteins are produced by granulosa cells of the follicle and provide a niche for follicle and oocyte growth [15,39].

Importantly, we found PAPP-A in FF was not active until tethering to the membrane GAG of fimbrial epithelial cells. This would provide a mechanism to conserve the growth activity of IGF until reaching the target. Indeed, we found depletion of PAPP-A from FF and blocking the membrane GAG-binding site both eliminated the transformation activity of FF toward fimbrial epithelial cells. PAPP-A has a molecular weight of ~800 kD in tetramer that cannot pass the 100 kD blood–follicle barrier [40]. It accumulates within the follicle with concentrations 500 times higher than in the serum [41]. Moreover, we found the transformation activities in different FFs highly correlated with levels of PAPP-A. Thus,

PAPP-A is the key determinant of the transformation activity of FF. Testing PAPP-A in FF and possibly in other tissue fluids may be applied to predict the risk of ovarian cancer.

Ovulation is a physiological process of acute inflammation. After LH surge, the ovulating follicle displays all of the hallmarks of acute inflammation [42] which ultimately leads to tissue degradation, cortex rupture, and release of the cumulus oophorus together with the follicular contents [43]. Upon oocyte pick-up, the fimbrial epithelium is injured by exposure to ovulatory contents. Previously, we found that undiluted or less diluted (50%) FF is highly toxic to fimbrial epithelial cells and tissue [12]. When examining different parts of the fallopian tube collected at various stages of the menstrual cycle, we found the fimbrial part, in contrast to the proximal part, carries much more ROS stress and DNA DSBs in the epithelial cells, specifically in those tubes collected around ovulation. Furthermore, in an IHC study of stemness markers on the fallopian tube epithelium, the highest proportion of stem cell markers was found in the distal part [44]. In this study, we provide evidence that FF-IGF is responsible for the induction of stemness in fimbrial epithelium on a sequence of AKT phosphorylation, OCT4 nuclear translocation, and NANOG expression. By this mechanism, injured epithelia of the fimbria and ovary can be repaired after ovulation.

Blocking the IGF2 receptor or the downstream self-renewal factor NANOG both largely reduced the transformation, suggesting the stem/progenitor cells are the origin of transformation. In the 3D spheroid colony forming experiment, FF-IGF largely increased the colony forming rate of both primary and p53/Rb-immortalized cells, suggesting ovulatory IGF acts both before and after the initiation of transformation. In the p53/Rb-initiated cells, FF-IGF further conferred expansion of the initiated clones. These cells readily form undifferentiated carcinoma in xenograft and shows a transformed karyotype with CNVs and aneuploidy.

Results of the present and our previous studies lead to an integrative mechanism of transformation of the fallopian tube fimbrial epithelium that fits to the two well-known epidemiological risk factors for ovarian cancer, ovulation and retrograde menstruation (Fig. 6b). High level of ROS in ovulatory FF induces DNA DSBs in the secretory cells of the fimbrium [12]. Cells stressed with this high ROS are normally subjected

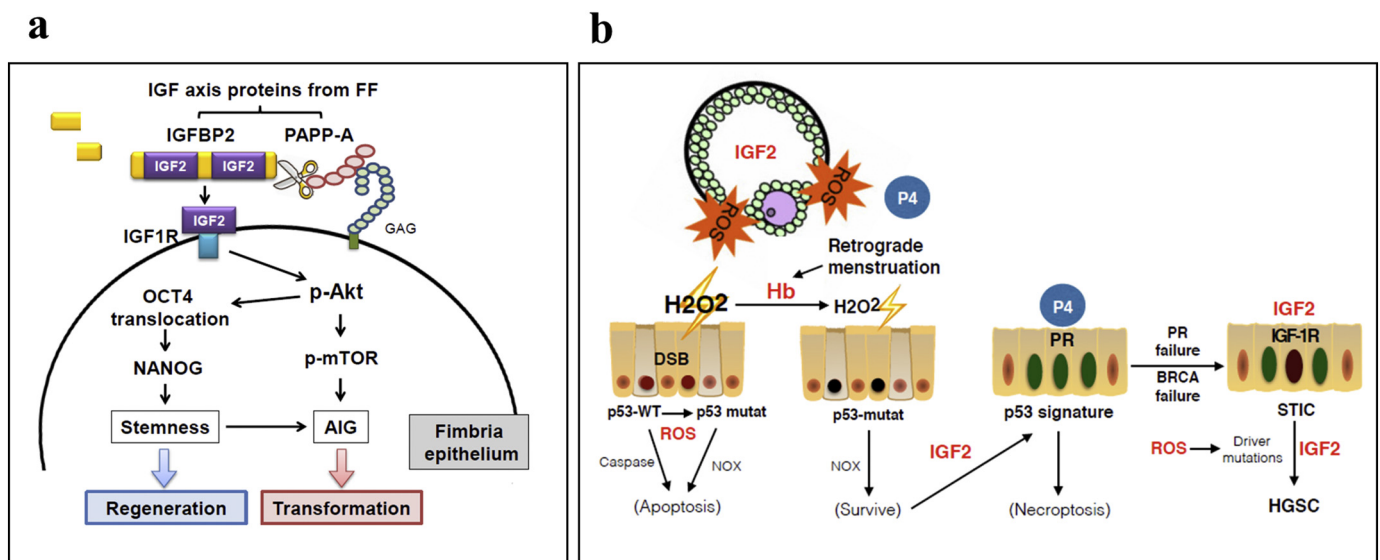


**Fig. 7.** An integrative mechanism of ovulation induced transformation of the fallopian tube fimbrial epithelium by IGF axis in FF. (a) A summary of regeneration and transformation of fallopian tube fimbrial epithelium by IGF axis in FF. Upon ovulation, fallopian tube fimbrial epithelium is exposed to IGF axis proteins. After tethering to the membrane GAG, PAPP-A cleaves IGFBP2 and releases IGF2 to bind with IGF-1R on fimbrial epithelial cells. Subsequent activation of the AKT/OCT4/NANOG and AKT/mTOR pathways leads to activation of stem cells to regenerate injured fimbrial epithelium, or clonal expansion and malignant transformation of initiated cancer cells. (b) Ovulatory ROS acts as the mutagen to induce DNA mutations such as double strand breaks (DSB) [12] and IGF acts as the stem cell growth factor to expand the mutant clone. By consuming H<sub>2</sub>O<sub>2</sub> extracellularly, hemoglobin (Hb) from retrograde menstruation rescues the ROS stressed cells from p53-mediated or, when p53 is lost, NOX-mediated apoptosis [16]. This allows expansion of TP53-mutated stem/progenitor cells to form the p53 signature. On the other hand, progesterone (P4) from luteinized follicle would induce necroptosis of TP53-mutated cells, effectively eradicates the precursor lesions [45]. It is up to the loss of progesterone receptor (PR), fails of homologous recombination repair proteins (BRCA1/2) as well as the incessant driving of mutagenesis and clonal expansion by ovulation that allows progression to STIC, and eventually metastasize to form the ovarian and peritoneal HGSC.

to apoptosis by p53-mediated or, when p53 is lost, by NOX-mediated stress responses. In the presence of hemoglobin in the pelvic cavity, most likely contributed by retrograde menstruation, the excessive ROS are consumed extracellularly and allow survival of the fimbrial epithelial cells while still accumulating DNA mutations [16,49]. With IGF axis in FF, the damaged cells regenerated soon after ovulation, while in TP53 mutated cells, IGF activates the stem cell clones and expand the cell population into the p53 signature lesion. Thus, ovulation provides the two principle driving forces of cancer evolution: ROS-mediated mutagenesis and IGF2 mediated stemness activation and clonal expansion. In addition, we discovered that the luteal phase progesterone could specifically eradicate p53-deficient fimbrial epithelial cells through induction of necroptosis [45]. Thus, the majority of HGSC have overcome this physiological protection by silencing PR [46]. Given that IGF-1R is highly expressed in fallopian tube epithelium and in the developed HGSC [47,48], neoplasm in the fimbria as well as in the ovary would receive this growth signal during each ovulation and would intermittently aggravate the disease (Fig. 7).

### Competing financial interests

The authors have declared that no conflict of interest exists.

### Author contributions

TYC, HSH conceived the project and obtained funding, TYC, CFH, and HSH designed experiments, CFH, HSH, DCD generated data; TYC, HSH and CFH interpreted data. PCC, TYC and DCD provided essential patient samples and clinical data; HSH, CFH, and TYC prepared the manuscript. All the authors provided a critical review of the manuscript.

### Conflict of interest

The authors have declared that no conflict of interest exists.

### Acknowledgments

The study was supported by grants of the Ministry of Science and Technology, Taiwan (MOST 106-2314-B-303-001-MY2; MOST 105-2314-B-303-017-MY2; MOST 107-2314-B-303-013-MY3), and Buddhist Tzu Chi General Hospital, Taiwan (TCMMP104-04-01).

### Appendix A. Supplementary data

Supplementary data to this article can be found online at <https://doi.org/10.1016/j.ebiom.2019.01.061>.

### References

- Siegel RL, Miller KD, Jemal A. Cancer statistics, 2016. *CA Cancer J Clin* 2016;66(1):7–30.
- Lee Y, Miron A, Drapkin R, Nucci MR, Medeiros F, Saleemuddin A, et al. A candidate precursor to serous carcinoma that originates in the distal fallopian tube. *J Pathol* 2007;211(1):26–35.
- Kuhn E, Wang TL, Doberstein K, Bahadiri-Talbot A, Ayhan A, Sehdev AS, et al. CCNE1 amplification and centrosome number abnormality in serous tubal intraepithelial carcinoma: further evidence supporting its role as a precursor of ovarian high-grade serous carcinoma. *Mod Pathol* 2016;29(10):1254–61.
- Meserve EEK, Brouwer J, Crum CP. Serous tubal intraepithelial neoplasia: the concept and its application. *Mod Pathol* 2017;30(5):710–21.
- McDaniel AS, Stall JN, Hovelson DH, Cani AK, Liu CJ, Tomlins SA, et al. Next-generation sequencing of tubal intraepithelial carcinomas. *JAMA Oncol* 2015;1(8):1128–32.
- Kuhn E, Kurman RJ, Vang R, Sehdev AS, Han G, Soslow R, et al. TP53 mutations in serous tubal intraepithelial carcinoma and concurrent pelvic high-grade serous carcinoma—evidence supporting the clonal relationship of the two lesions. *J Pathol* 2012;226(3):421–6.
- Kurman RJ, Shih Le M. The dualistic model of ovarian carcinogenesis: revisited, revised, and expanded. *Am J Pathol* 2016;186(4):733–47.
- Troisi R, Borge T, Gissler M, Grotmol T, Kitahara CM, Myrteit Saether SM, et al. The role of pregnancy, perinatal factors and hormones in maternal cancer risk: a review of the evidence. *J Intern Med* 2018;283(5):430–45.
- Jordan SJ, Cushing-Haugen KL, Wicklund KG, Doherty JA, Rossing MA. Breast-feeding and risk of epithelial ovarian cancer. *Cancer Causes Control* 2012;23(6):919–27.
- Havrilesky LJ, Moorman PG, Lowery WJ, Gierisch JM, Coeytaux RR, Urrutia RP, et al. Oral contraceptive pills as primary prevention for ovarian cancer: a systematic review and meta-analysis. *Obstet Gynecol* 2013;122(1):139–47.
- Beral V, Doll R, Hermon C, Peto R, Reeves G. Ovarian cancer and oral contraceptives: collaborative reanalysis of data from 45 epidemiological studies including 23,257 women with ovarian cancer and 87,303 controls. *Lancet* 2008;371(9609):303–14.
- Huang HS, Chu SC, Hsu CF, Chen PC, Ding DC, Chang MY, et al. Mutagenic, surviving and tumorigenic effects of follicular fluid in the context of p53 loss: initiation of fimbria carcinogenesis. *Carcinogenesis* 2015;36(11):1419–28.
- Lau A, Kollara A, St John E, Tone AA, Virtanen C, Greenblatt EM, et al. Altered expression of inflammation-associated genes in oviductal cells following follicular fluid exposure: implications for ovarian carcinogenesis. *Exp Biol Med (Maywood)* 2014;239(1):24–32.
- Bahar-Shany K, Brand H, Sapoznik S, Jacob-Hirsch J, Yung Y, Korach J, et al. Exposure of fallopian tube epithelium to follicular fluid mimics carcinogenic changes in precursor lesions of serous papillary carcinoma. *Gynecol Oncol* 2014;132(2):322–7.
- Emori MM, Drapkin R. The hormonal composition of follicular fluid and its implications for ovarian cancer pathogenesis. *Reprod Biol Endocrinol* 2014;12:60.
- Huang HS, Hsu CF, Chu SC, Chen PC, Ding DC, Chang MY, et al. Haemoglobin in pelvic fluid rescues fallopian tube epithelial cells from reactive oxygen species stress and apoptosis. *J Pathol* 2016;240(4):484–94.
- Paik DY, Janzen DM, Schafenacker AM, Velasco VS, Shung MS, Cheng D, et al. Stem-like epithelial cells are concentrated in the distal end of the fallopian tube: a site for injury and serous cancer initiation. *Stem Cells* 2012;30(11):2487–97.
- Karst AM, Drapkin R. Primary culture and immortalization of human fallopian tube secretory epithelial cells. *Nat Protoc* 2012;7(9):1755–64.
- Donehower LA, Harvey M, Slagle BL, McArthur MJ, Montgomery Jr CA, Butel JS, et al. Mice deficient for p53 are developmentally normal but susceptible to spontaneous tumours. *Nature* 1992;356(6366):215–21.
- Clemmons DR. IGF binding proteins and their functions. *Mol Reprod Dev* 1993;35(4):368–74 [discussion 74–5].
- Sun IY, Overgaard MT, Oxvig C, Giudice LC. Pregnancy-associated plasma protein a proteolytic activity is associated with the human placental trophoblast cell membrane. *J Clin Endocrinol Metab* 2002;87(11):5235–40.
- Laursen LS, Overgaard MT, Weyer K, Boldt HB, Ebbesen P, Christiansen M, et al. Cell surface targeting of pregnancy-associated plasma protein a proteolytic activity. Reversible adhesion is mediated by two neighboring short consensus repeats. *J Biol Chem* 2002;277(49):47225–34.
- Fathalla MF. Incessant ovulation—a factor in ovarian neoplasia? *Lancet* 1971;2(7716):163.
- Fathalla MF. Incessant ovulation and ovarian cancer - a hypothesis re-visited. *Facts Views Vis ObGyn* 2013;5(4):292–7.
- Mosieniak G, Sikora E. Polyploidy: the link between senescence and cancer. *Curr Pharm Des* 2010;16(6):734–40.
- Eguchi T, Takaki T, Itadani H, Kotani H. RB silencing compromises the DNA damage-induced G2/M checkpoint and causes deregulated expression of the ECT2 oncogene. *Oncogene* 2007;26(4):509–20.
- Bielski CM, Zehir A, Penson AV, Donoghue MTA, Chatila W, Armenia J, et al. Genome doubling shapes the evolution and prognosis of advanced cancers. *Nat Genet* 2018;50(8):1189–95.
- Karst AM, Jones PM, Vena N, Ligon AH, Liu JF, Hirsch MS, et al. Cyclin E1 deregulation occurs early in secretory cell transformation to promote formation of fallopian tube-derived high-grade serous ovarian cancers. *Cancer Res* 2014;74(4):1141–52.
- Lv L, Zhang T, Yi Q, Huang Y, Wang Z, Hou H, et al. Tetraploid cells from cytokinesis failure induce aneuploidy and spontaneous transformation of mouse ovarian surface epithelial cells. *Cell Cycle* 2012;11(15):2864–75.
- Schouten LJ, Rivera C, Hunter DJ, Spiegelman D, Adami HO, Arslan A, et al. Height, body mass index, and ovarian cancer: a pooled analysis of 12 cohort studies. *Cancer Epidemiol Biomark Prev* 2008;17(4):902–12.
- Lango Allen H, Estrada K, Lettre G, Berndt SI, Weedon MN, Rivadeneira F, et al. Hundreds of variants clustered in genomic loci and biological pathways affect human height. *Nature* 2010;467(7317):832–8.
- Baumgarten SC, Convisar SM, Fierro MA, Winston NJ, Scoccia B, Stocco C. IGF1R signaling is necessary for FSH-induced activation of AKT and differentiation of human cumulus granulosa cells. *J Clin Endocrinol Metab* 2014;99(8):2995–3004.
- el-Roeiy A, Chen X, Roberts VJ, LeRoith D, Roberts Jr CT, Yen SS. Expression of insulin-like growth factor-I (IGF-I) and IGF-II and the IGF-I, IGF-II, and insulin receptor genes and localization of the gene products in the human ovary. *J Clin Endocrinol Metab* 1993;77(5):1411–8.
- Qu J, Godin PA, Nisolle M, Donnez J. Expression of receptors for insulin-like growth factor-I and transforming growth factor-beta in human follicles. *Mol Hum Reprod* 2000;6(2):137–45.
- Klein NA, Battaglia DE, Woodruff TK, Padmanabhan V, Giudice LC, Bremner WJ, et al. Ovarian follicular concentrations of activin, follistatin, inhibin, insulin-like growth factor I (IGF-I), IGF-II, IGF-binding protein-2 (IGFBP-2), IGFBP-3, and vascular endothelial growth factor in spontaneous menstrual cycles of normal women of advanced reproductive age. *J Clin Endocrinol Metab* 2000;85(12):4520–5.
- Seifer DB, Giudice LC, Dsupin BA, Haning Jr RV, Frishman GN, Burger HG. Follicular fluid insulin-like growth factor-I and insulin-like growth factor-II concentrations vary as a function of day 3 serum follicle stimulating hormone. *Hum Reprod* 1995;10(4):804–6.

- [37] Monget P, Mazerbourg S, Delpuech T, Maurel MC, Maniere S, Zapf J, et al. Pregnancy-associated plasma protein-a is involved in insulin-like growth factor binding protein-2 (IGFBP-2) proteolytic degradation in bovine and porcine preovulatory follicles: identification of cleavage site and characterization of IGFBP-2 degradation. *Biol Reprod* 2003;68(1):77–86.
- [38] Bach LA. Recent insights into the actions of IGFBP-6. *J Cell Commun Signal* 2015;9(2):189–200.
- [39] Jepsen MR, Klooverpris S, Botkjaer JA, Wissing ML, Andersen CY, Oxvig C. The proteolytic activity of pregnancy-associated plasma protein-a is potentially regulated by stanniocalcin-1 and -2 during human ovarian follicle development. *Hum Reprod* 2016;31(4):866–74.
- [40] Shalgi R, Kraicer P, Rimon A, Pinto M, Soferman N. Proteins of human follicular fluid: the blood-follicle barrier. *Fertil Steril* 1973;24(6):429–34.
- [41] Rezabek K, Moosova M, Pavelkova J, Moos J, Filova V. Follicular fluid and serum concentrations of PAPP-A in OHSS risk group of women undergoing IVF stimulation. *Ceska Gynekol* 2009;74(2):80–4.
- [42] Espey LL. Current status of the hypothesis that mammalian ovulation is comparable to an inflammatory reaction. *Biol Reprod* 1994;50(2):233–8.
- [43] Sirois J, Sayasith K, Brown KA, Stock AE, Bouchard N, Dore M. Cyclooxygenase-2 and its role in ovulation: a 2004 account. *Hum Reprod Update* 2004;10(5):373–85.
- [44] Auersperg N. The stem-cell profile of ovarian surface epithelium is reproduced in the oviductal fimbriae, with increased stem-cell marker density in distal parts of the fimbriae. *Int J Gynecol Pathol* 2013;32(5):444–53.
- [45] Wu NY, Huang HS, Chao TH, Chou HM, Fang C, Qin CZ, et al. Progesterone prevents high-grade serous ovarian Cancer by inducing Necroptosis of p53-defective fallopian tube epithelial cells. *Cell Rep* 2017;18(11):2557–65.
- [46] Tone AA, Virtanen C, Shaw PA, Brown TJ. Decreased progesterone receptor isoform expression in luteal phase fallopian tube epithelium and high-grade serous carcinoma. *Endocr Relat Cancer* 2011;18(2):221–34.
- [47] Pfeifer TL, Chegini N. Immunohistochemical localization of insulin-like growth factor (IGF-I), IGF-I receptor, and IGF binding proteins 1-4 in human fallopian tube at various reproductive stages. *Biol Reprod* 1994;50(2):281–9.
- [48] Spentzos D, Cannistra SA, Grall F, Levine DA, Pillay K, Libermann TA, et al. IGF axis gene expression patterns are prognostic of survival in epithelial ovarian cancer. *Endocr Relat Cancer* 2007;14(3):781–90.
- [49] Lin SF, Gerry E, Shih IM. Tubal origin of ovarian cancer - the double-edged sword of haemoglobin. *J Pathol* 2017 May;242(1):3–6.